

AD/A-001 135

AERODYNAMIC HEATING OF SUPERSONIC
BLUNT BODIES

David C. Chou, et al

Iowa University

Prepared for:

Army Research Office-Durham

September 1974

DISTRIBUTED BY:

NTIS

National Technical Information Service
U. S. DEPARTMENT OF COMMERCE

AERODYNAMIC HEATING OF SUPERSONIC BLUNT BODIES

David C. Chou

and

Theodore F. Smith

Division of Energy Engineering
College of Engineering
The University of Iowa
Iowa City, Iowa 52242

September, 1974

Reproduced by
NATIONAL TECHNICAL
INFORMATION SERVICE
U. S. Department of Commerce
Springfield, VA 22151

Final report submitted to
U. S. Army Research Office
Box CM Duke Station
Durham, North Carolina 27706
Contract No. DAHC04-74-G-0097

UNCLASSIFIED

SECURITY CLASSIFICATION OF THIS PAGE (When Data Entered)

REPORT DOCUMENTATION PAGE		READ INSTRUCTIONS BEFORE COMPLETING FORM
1. REPORT NUMBER E-DCC-74-001	2. GOVT ACCESSION NO.	3. RECIPIENT'S CATALOG NUMBER
4. TITLE (and Subtitle) Aerodynamic heating of supersonic blunt bodies		5. TYPE OF REPORT & PERIOD COVERED Final Report 7 Jan. 74 to 31 Aug. 74
		6. PERFORMING ORG. REPORT NUMBER
7. AUTHOR(s) David C. Chou and Theodore F. Smith		8. CONTRACT OR GRANT NUMBER(s) DAHC04-74-G-0097
9. PERFORMING ORGANIZATION NAME AND ADDRESS Division of Energy Engineering College of Engineering, The University of Iowa Iowa City, Iowa 52242		10. PROGRAM ELEMENT, PROJECT, TASK AREA & WORK UNIT NUMBERS
11. CONTROLLING OFFICE NAME AND ADDRESS U. S. Army Research Office Box CM Duke Station Durham, North Carolina 27706		12. REPORT DATE September 1974
		13. NUMBER OF PAGES
14. MONITORING AGENCY NAME & ADDRESS (if different from Controlling Office) Unclassified		15. SECURITY CLASS. (of this report) Unclassified
		15a. DECLASSIFICATION/DOWNGRADING SCHEDULE
16. DISTRIBUTION STATEMENT (of this Report)		
17. DISTRIBUTION STATEMENT (of the abstract entered in Block 20, if different from Report)		
18. SUPPLEMENTARY NOTES		
19. KEY WORDS (Continue on reverse side if necessary and identify by block number) aerodynamic, heat transfer, boundary-layer, mathematical model		
20. ABSTRACT (Continue on reverse side if necessary and identify by block number) The object of this research is to investigate the rate of aerodynamic heat transfer on the surface of a blunt body of revolution flying at supersonic speed. A mathematical model, based on Illingworth-Stewartson transformation and a perturbation technique with a similarity analysis, which describes the aerodynamic heating processes associated with supersonic flight of a blunt-nose projectile has been developed. The governing transport equations are reduced to a set of coupled nonlinear ordinary differential equations in first, third, and fifth order of the transformed coordinates. The equations were solved by a standard		

DD FORM 1473

EDITION OF 1 NOV 65 IS OBSOLETE
S/N 0103-014-6601

UNCLASSIFIED

SECURITY CLASSIFICATION OF THIS PAGE (When Data Entered)

UNCLASSIFIED

SECURITY CLASSIFICATION OF THIS PAGE(When Data Entered)

numerical integration scheme. Results describing velocity and temperature, profiles inside the boundary layer, skin friction and local heat transfer rates are presented.

11
UNCLASSIFIED

SECURITY CLASSIFICATION OF THIS PAGE(When Data Entered)

ACKNOWLEDGMENTS

This research was sponsored by the U. S. Army Research Office under Contract No. DAHC04-74-G-0097. The U. S. Army representative who directed this contract was Mr. Darrel M. Thomsen, Research Directorate, General Thomas J. Rodman Laboratory, Rock Island Arsenal, Rock Island, Illinois.

The authors wish to acknowledge Mr. Shakil Mohamed who assisted in the numerical calculations and presentation of results. A portion of computer funds used in this research was supplied by the Graduate College. The assistance of the Publications Office of the College of Engineering for preparing this report is gratefully acknowledged.

TABLE OF CONTENTS

	Page
LIST OF FIGURES	v
LIST OF TABLES	v
NOMENCLATURE	vi
1. INTRODUCTION	1
2. ANALYSIS	3
2.1 Governing equations	3
2.2 Boundary layer characteristics	5
3. METHOD OF SOLUTION	14
4. DISCUSSION OF RESULTS	16
4.1 Solutions of governing equations	16
4.2 Results for boundary layer characteristics	22
5. CONCLUSIONS	31
6. REFERENCES	33
APPENDIX A	34

LIST OF FIGURES

	Page
Figure 4.1 First-order perturbation results	13
Figure 4.2 Third-order perturbation results	19
Figure 4.3 Fifth-order perturbation results, first set of equations	20
Figure 4.4 Fifth-order perturbation results, second set of equations	21
Figure 4.5 Velocity and temperature profiles ($M_\infty = 1.5$, $\gamma = 1.4$)	23
Figure 4.6 Surface shear stress ($M_\infty = 1.5$, $\gamma = 1.4$)	25
Figure 4.7 Reynolds number-shear stress parameter ($M_\infty = 1.5$, $\gamma = 1.4$)	27
Figure 4.8 Heat transfer and Nusselt number ($M_\infty = 1.5$, $\gamma = 1.4$)	28
Figure 4.9 Reynolds analogy parameter ($M_\infty = 1.5$, $\gamma = 1.4$)	30

LIST OF TABLES

Table 4.1 Wall derivatives for velocity and temperature functions	17
Table A.1 Computer program AER	35
Table A.2 Computer program AERL	44

NOMENCLATURE

b	Dynamic viscosity coefficient
c	Velocity of sound
C_f	Friction coefficient
\bar{d}	Transformed coordinate
D	Body diameter
f_1, g_3, g_5, h_5	Velocity functions
g	Parameter defined in Eq. (2.8)
h	Convective heat transfer coefficient
j, \bar{j}	Parameters defined in Eq. (2.17)
k	Thermal conductivity
M_∞	Mach number
Nu	Nusselt number
P	Pressure
Pr	Prandtl number
q	Heat flux
Re	Reynolds number
\bar{s}_1, \bar{s}_2	Parameters defined in Eq. (2.7)
S	Relative enthalpy difference
s_0, z_2, z_4, w_4	Temperature functions
T	Temperature
u	Tangential velocity
u_1, u_3, u_5	Coefficients of velocity series
U	Boundary layer edge velocity
x, \bar{x}	Coordinates along body surface

x	Transformed coordinate
y	Coordinate normal to body surface
α	Angle
$\beta, \bar{\beta}$	Velocity parameters defined in Eqs. (2.7) and (2.9)
γ	Specific heat ratio
η	Similar independent variable
μ	Dynamic viscosity
ν	Kinematic viscosity
ρ	Density
τ	Shear stress

Subscripts

0	Stagnation
1	Boundary layer edge
w	Wall

I. INTRODUCTION

Aerodynamic heating of a blunt body is a result of flow of air at high speed about it. Direct compression and internal friction at and near the stagnation regions of forward surfaces of the body convert the kinetic energy of motion into heat within the boundary layer of air which surrounds the body. Consequently, aerodynamic heating problems dictate the design of blunt bodies, not only for structural reasons, but also because of thermal problems associated with protecting vital internal components, such as electronic packages which are usually located in the forward part of the body.

Previous investigations concerning aerodynamic heating problems have concentrated in the area of high supersonic or hypersonic flows at high altitude low density atmospheric flight, such as in entry or re-entry cases.[1]* However, current interest in blunt bodies which fly at moderate supersonic speeds, but in the dense low altitude atmosphere, call for further investigation in aerodynamic heating problems characterized by relatively lower Mach and Reynolds numbers. The objective of this study is primarily to obtain heat transfer coefficients and recovery factors along the forward surfaces of the body to allow for coupling these parameters into a complete heat-transfer analysis inside the body. This information can be obtained by solving a three-dimensional, compressible boundary layer around a body with a blunt nose, which may or may not have an additional rotating speed complication.

* Bracketed numbers refer to entries in REFERENCES.

The basic nonlinear partial differential equations [2] which govern the motion of a steady, axisymmetric, compressible nonrotating laminar boundary layer flow about a body of revolution have been transformed into a more convenient form by a modified Illingworth-Stewartson transformation [3]. A special procedure to relate the physical sensible external flow conditions with the transformed ones was presented. Similarity variables were found by applying the systematic one-parameter group theory. The simplified governing equations were then transformed again by the well-known similar analysis [3]. A perturbation scheme based on the transformed coordinates was constructed to render a series of coupled nonlinear ordinary differential equations which are readily solved by standard numerical integration subroutines to provide the desirable flow property distributions, including heat transfer rates. The purposes of this report are to present solutions to the differential equations and to examine velocity and temperature profiles within the boundary layers as well as shear stresses and heat transfer rates at the surface of the body.

2. ANALYSIS

2.1 Governing equations

The basic nonlinear partial differential equations which describe mass, momentum and energy transport for steady, axisymmetric, compressible, nonrotating laminar boundary layer flow about a body of revolution have been transformed into a series of coupled nonlinear ordinary differential equations. Details describing this analysis are presented elsewhere [3] and are not cited here. For convenience, however, only the ordinary differential equations are presented. These equations are given, after some modification, from those previously reported [3]

$$\begin{aligned} \bar{x}: \quad f_1''' &= -2 f_1 f_1'' + f_1'^2 - 1 - S_0 \\ S_0' &= -2 f_1 S_0' \end{aligned} \quad \left. \vphantom{\begin{aligned} \bar{x}: \quad f_1''' &= -2 f_1 f_1'' + f_1'^2 - 1 - S_0 \\ S_0' &= -2 f_1 S_0' \end{aligned}} \right\} (2.1)$$

$$\begin{aligned} \bar{x}^3: \quad g_3''' &= -2 f_1 g_3'' + 4 f_1' g_3' - 4 f_1'' g_3 - 2 f_1 f_1'' \\ &\quad - 4(1 + S_0) - z_2 \\ z_2' &= -2 f_1 z_2' + 2 f_1' z_2 - 2(2 g_3 + f_1) S_0' \end{aligned} \quad \left. \vphantom{\begin{aligned} \bar{x}^3: \quad g_3''' &= -2 f_1 g_3'' + 4 f_1' g_3' - 4 f_1'' g_3 - 2 f_1 f_1'' \\ &\quad - 4(1 + S_0) - z_2 \\ z_2' &= -2 f_1 z_2' + 2 f_1' z_2 - 2(2 g_3 + f_1) S_0' \end{aligned}} \right\} (2.2)$$

$$\begin{aligned} \bar{x}^5: \quad g_5''' &= -2 f_1 g_5'' + 6 f_1' g_5' - 6 f_1'' g_5 - 4 f_1 f_1'' \\ &\quad - 6(1 + S_0) - z_4 \\ z_4' &= -2 f_1 z_4' + 4 f_1' z_4 - 6 S_0' g_5 - 4 f_1 S_0' \end{aligned} \quad \left. \vphantom{\begin{aligned} \bar{x}^5: \quad g_5''' &= -2 f_1 g_5'' + 6 f_1' g_5' - 6 f_1'' g_5 - 4 f_1 f_1'' \\ &\quad - 6(1 + S_0) - z_4 \\ z_4' &= -2 f_1 z_4' + 4 f_1' z_4 - 6 S_0' g_5 - 4 f_1 S_0' \end{aligned}} \right\} (2.3)$$

$$\begin{aligned}
 h_5''' &= -2f_1 h_5'' + 6f_1' h_5' - 6f_1'' h_5 + 3g_3'^2 - 4g_3 g_3'' \\
 &\quad - 2f_1' g_3 - 2f_1 g_3'' + 2f_1 f_1'' - 3(1 + s_0) \\
 &\quad - 4z_2 - w_4 \\
 w_4' &= -2f_1 w_4' + 4f_1' w_4 + 2g_3' z_2 - 4g_3 z_2' - 2f_1 z_2' \\
 &\quad - 6s_0' h_5 - 2s_0' g_3 + 2f_1 s_0'
 \end{aligned}
 \tag{2.4}$$

with corresponding boundary conditions

$$\begin{aligned}
 \eta = 0: & \quad f_1 = 0 & g_3 = 0 & g_5 = 0 & h_5 = 0 \\
 & f_1' = 0 & g_3' = 0 & g_5' = 0 & h_5' = 0 \\
 & s_0' = 0 & z_2' = 0 & z_4' = 0 & w_4' = 0 \\
 \text{or} & \quad s_0 = s_w & z_2 = 0 & z_4 = 0 & w_4 = 0
 \end{aligned}
 \tag{2.5}$$

$$\begin{aligned}
 \eta = \infty: & \quad f_1' = 1 & g_3' = 1 & g_5' = 1 & h_5' = 0 \\
 & s_0 = 0 & z_2 = 0 & z_4 = 0 & w_4 = 0
 \end{aligned}
 \tag{2.6}$$

Solution of these differential equations with associated boundary conditions is presented in Chapter 3 with results discussed in Chapter 4.

2.2 Boundary layer characteristics

Once solutions to the ordinary differential equations given in Sec. 2.1 are available, quantities such as velocity and temperature profiles within the boundary layer as well as shear stresses and heat transfer rates at the surface of the body can be evaluated. The purpose of this section is to present expressions which may be utilized to evaluate these quantities as well as others that are generally employed to describe boundary layer characteristics. It is convenient to introduce certain dimensionless variables which allow presentation of results and discussion to be considerably simplified. Examination of definitions and expressions for transformed variables, stream function and relative enthalpy difference as presented in Ref. [3] reveals that the following dimensionless variables can be defined in terms of the previously introduced parameters.

$$\begin{aligned}
 \bar{x} &= x/D, & \bar{\beta} &= \beta D/c_0, & \bar{j} &= jD^2 = \frac{\gamma-1}{2} \beta^2 \\
 \bar{d} &= \tilde{x}/bD \\
 \bar{s}_1 &= \frac{u_3 b^2 D^2}{u_1} = \frac{\bar{j}(2g+3)}{6} \\
 \bar{s}_2 &= \frac{u_5 b^4 D^4}{u_1} = \frac{\bar{j}^2(28g^2 + 72g + 45)}{120}
 \end{aligned}
 \tag{2.7a-f}$$

where

$$g = \frac{3\gamma - 1}{2(\gamma - 1)} \tag{2.8}$$

$\bar{\beta}$ is expressed as

$$\bar{\beta} = M_{\infty} \left\{ \frac{3[(\gamma - 1) M_{\infty}^2 + 2]}{(\gamma + 1) M_{\infty}^2} \left[1 + \frac{\gamma + 1}{2} \frac{(\gamma - 1) M_{\infty}^2 + 2}{2\gamma M_{\infty}^2 - (\gamma - 1)} \right]^{-[1/(\gamma - 1)]} \right\} \quad (2.9)$$

Employing the above dimensionless variables, the distance along the surface measured from the tip of the blunt body is expressed as

$$\bar{x} = \bar{d} + \bar{d}^3 \frac{\bar{j}g}{3} + \bar{d}^5 \bar{j}^2 g \frac{(7g + 3)}{30} \quad (2.10a)$$

For positions near the tip of the body, \bar{d} is small and Eq. (2.4) reduces to

$$\bar{x} = \bar{d} \quad (2.10b)$$

Because of the method employed in the analysis to describe the boundary layer edge velocity, \bar{x} is limited to values less than about 0.611 which corresponds to an angle α as defined in Ref. [3] of 35° . The maximum value of the transformed coordinate \bar{d} is dependent on the limiting value of \bar{x} . In terms of \bar{x} , \bar{d} can be written as

$$\bar{d} = \bar{x} - \bar{x}^3 \frac{\bar{j}g}{3} + \bar{x}^5 \bar{j}^2 g \frac{(g - 1)}{10} \quad (2.11)$$

In expressing Eqs. (2.10) and (2.11), up to the fifth order results were retained in the perturbation scheme [3]. Similar expressions for the distance measured normal to the body surface can be developed but are not presented here.

In most applications, the tangential velocity component within the boundary layer is of interest since its gradient determines the drag experienced by the body as it passes through a gas. Consequently, only results for the tangential velocity are presented. Expression for the normal velocity component may be developed using the definitions as reported in Ref. [3]. Utilizing the definitions for the stream function as well as for the boundary layer edge velocity, the normal velocity component is expressed as

$$\frac{u}{U_1} = \frac{f_1' + \tilde{d}^2 \bar{s}_1 g_3' + \tilde{d}^4 (\bar{s}_2 g_5' + \bar{s}_1^2 h_5')}{1 + \tilde{d}^2 \bar{s}_1 + \tilde{d}^4 \bar{s}_2} \quad (2.12a)$$

where U_1 represents the boundary layer edge velocity. Velocity functions f_1 , g_3 , g_5 and h_5 are solutions to the ordinary differential equations and are understood to be dependent on the similar independent variable η . At a sufficiently large value of η corresponding to the boundary layer edge, the velocity ratio in Eq. (2.12a) attains a value of unity. For small values of \tilde{d} , this ratio is given by

$$\frac{u}{U_1} = f_1'(\eta) \quad (2.12b)$$

which is a solution to Eq. (2.1). At the surface of the body where $\eta = 0$, the velocity ratio is zero as can be observed by imposing the boundary conditions given in Eq. (2.5).

Temperature profile within the boundary layer is determined from the definition of the relative enthalpy difference [3]. After some

manipulations and recognizing the dimensionless variables, the gas temperature normalized with the free stream stagnation temperature is written as

$$\frac{T}{T_0} = (S + 1) - \frac{\gamma - 1}{2} (\bar{\beta}\bar{x})^2 \left(\frac{u}{U_1} \right)^2 \quad (2.13a)$$

The relative enthalpy difference S introduced in Eq. (2.13) is given in terms of solutions to the differential equations as

$$S = S_0 + \bar{d}^2 \bar{s}_1 z_2 + \bar{d}^4 (\bar{s}_2 z_4 + \bar{s}_1^2 w_4) \quad (2.14)$$

where temperature functions S_0 , z_2 , z_4 and w_4 are functions of η . On the surface of the body, Eq. (2.13) reduces to

$$\frac{T_w}{T_0} = S_w + 1 \quad (2.15)$$

where T_w is surface temperature which may vary with \bar{x} . Values of S_w less than zero correspond to cooled surface $T_w/T_0 < 1$ and greater than zero to a heated surface $T_w/T_0 > 1$. At the boundary layer edge, $S = 0$ by boundary conditions cited in Eq. (2.6) and the temperature is

$$\frac{T_1}{T_0} = 1 - \frac{\gamma - 1}{2} (\bar{\beta}\bar{x})^2 \quad (2.16)$$

where subscript "1" refers to the boundary layer edge. Thus, the boundary layer edge temperature is just a function of \bar{x} and free stream Mach number. In the analysis [3], the Prandtl number was assigned a

value of unity. Hence, the adiabatic wall boundary condition yields $S = 0$ within the boundary layer which implies that the temperature distribution is solely dependent on the tangential velocity distribution for a given \bar{x} position [4]. This can be observed by substituting a value of zero for S in Eq. (2.13a). In addition, the wall temperature for $Pr = 1$ with adiabatic boundary condition equals the free stream stagnation temperature and the recovery factor is unity [5]. For sufficiently small values of \tilde{d} , Eq. (2.13) may be written as

$$\frac{T}{T_0} = S_0(\eta) + 1 \quad (2.13b)$$

where it was further assumed that the velocity is small. This is justifiable since small values of \tilde{d} correspond to the stagnation region of the blunt body where the velocities are small.

Shear stress at the body surface indicates the drag on the body and is evaluated from the following expression

$$\tau_w = \mu_w \left. \frac{\partial u}{\partial y} \right|_w = \sqrt{b\mu_0\gamma P_0\beta} \bar{\beta}\bar{x} \cdot \left(\frac{T_1}{T_0} \right)^8 \frac{[f_1' + \tilde{d}^2 \bar{s}_1 g_3' + \tilde{d}^4 (\bar{s}_2 g_5' + \bar{s}_1^2 h_5')]_{\eta=0}}{1 + \tilde{d}^2 \bar{s}_1 + \tilde{d}^4 \bar{s}_2} \quad (2.17a)$$

Second derivatives of the velocity functions are thus related to the shear stress. Equation (2.17) reduces to the following for small values of \tilde{d}

$$\tau_w = \sqrt{b\mu_0\gamma P_0\beta} \bar{\beta}\bar{x} f_1''(0) \quad (2.17b)$$

Another quantity of interest is skin friction coefficient given by

$$C_f = \frac{\tau_w}{\frac{1}{2} \rho_w U_1^2} = \frac{2(S_w + 1)}{\tilde{d}} \sqrt{\frac{v_0}{u_1 D^2}} \cdot \frac{[f_1'' + \tilde{d}^2 \bar{s}_1 g_3'' + \tilde{d}^4 (\bar{s}_2 g_5'' + \bar{s}_1^2 h_5'')]_{\eta=0}}{(1 + \tilde{d}^2 \bar{s}_1 + \tilde{d}^4 \bar{s}_2)^2} \quad (2.18a)$$

For small values of \tilde{d} , skin friction coefficient is

$$C_f = \frac{2(S_w + 1)}{\tilde{d}} \sqrt{\frac{v_0}{u_1 D^2}} f_1''(0) \quad (2.18b)$$

Finally, the Reynolds number-skin friction parameter is expressed as

$$\frac{C_f \sqrt{Re_w}}{2} = \sqrt{\frac{d \ln \tilde{d}}{d \ln x}} \cdot \frac{[f_1'' + \tilde{d}^2 \bar{s}_1 g_3'' + \tilde{d}^4 (\bar{s}_2 g_5'' + \bar{s}_1^2 h_5'')]_{\eta=0}}{(1 + \tilde{d}^2 \bar{s}_1 + \tilde{d}^4 \bar{s}_2)^{3/2}} \quad (2.19a)$$

where

$$\frac{d \ln \tilde{d}}{d \ln x} = \frac{1 + \tilde{d}^2 \bar{j} g/3 + \tilde{d}^4 \bar{j}^2 g(7g+3)/30}{1 + \tilde{d}^2 \bar{j} g + \tilde{d}^4 \bar{j}^2 g(7g+3)/6} \quad (2.20)$$

The Reynolds number introduced in Eq. (2.19) is defined as

$$Re = U_1 x / \nu_w \quad (2.21)$$

where all properties are evaluated at the body surface. Near the stagnation region of the blunt body, this parameter assumes the form

$$\frac{C_f \sqrt{Re_w}}{2} = f_1''(0) \quad (2.19b)$$

Heat flux at the body surface is evaluated from

$$q = -k_w \left. \frac{\partial T}{\partial y} \right|_w = -k_w T_0 \sqrt{\frac{u_1}{\nu_0}} \left(\frac{T_1}{T_0} \right)^{\frac{1}{2}} \frac{1}{S_w + 1} S'(0) \quad (2.22a)$$

where $S'(0)$ is found by taking derivative of Eq. (2.14) with respect to η and evaluating at $\eta = 0$. Thus, heat transfer is related to first derivatives of the temperature functions. For small δ values, Eq. (2.22) is written as

$$q = -k_w T_0 \sqrt{\frac{u_1}{\nu_0}} \frac{1}{S_w + 1} S'_0(0) \quad (2.22b)$$

Positive and negative values of heat flux imply heating and cooling of the surface, respectively. The boundary condition with $S'(0) = 0$ yields a zero heat flux which corresponds to adiabatic or insulated wall. A convective heat transfer coefficient can be defined as follows

$$q = h(T_w - T_0) \quad (2.23)$$

where the free stream stagnation temperature has been employed. Several other definitions [4,5] employ the adiabatic wall temperature which is the temperature acquired by an adiabatic surface. However, for the existing analysis with $Pr = 1$, the adiabatic and free stream temperatures are identical. The local Nusselt number can then be written as

$$Nu = \frac{hx}{k_w} = - \frac{\sqrt{Re_w}}{S_w} \sqrt{\frac{d}{d} \frac{\ln d}{\ln x}} \frac{S'(0)}{(1 + \tilde{d}^2 \bar{s}_1 + \tilde{d}^4 \bar{s}_2)^{1/2}} \quad (2.24a)$$

This expression reduces to the following form for small values of \tilde{d}

$$Nu = - \frac{\sqrt{Re_w}}{S_w} S'_0(0) \quad (2.24b)$$

The dependency of the Nusselt number on the Reynolds number as displayed in Eq. (2.24) is similar to that observed for a flat plate, cylinder or sphere for laminar boundary layer flow [6].

A final parameter that is useful in examining boundary layer characteristics is the Reynolds analogy parameter which for the present analysis acquires the form

$$\frac{C_f Re_w}{2Nu} = - \frac{S_w [f_1'' + \tilde{d}^2 \bar{s}_1 g_3'' + \tilde{d}^4 (\bar{s}_2 g_5'' + \bar{s}_1^2 h_5'')]_{\eta=0}}{(1 + \tilde{d}^2 \bar{s}_1 + \tilde{d}^4 \bar{s}_2)^{1/2} S'(0)} \quad (2.25a)$$

For small values of \tilde{d} , this parameter reduces to

$$\frac{C_f Re_w}{2Nu} = - \frac{S_w f_1''(0)}{S'_0(0)} \quad (2.25b)$$

The Reynolds analogy parameter illustrates the interrelationship between fluid friction and heat transfer processes. If the Prandtl number is included in this parameter, then the dimensionless grouping of $Nu/Re_w Pr$ is known as the Stanton number. Laminar boundary layer on a flat plate with zero pressure gradient yields a value of one for the Reynolds analogy parameter [7].

3. METHOD OF SOLUTION

The method employed to obtain solutions to the ordinary differential equations as given in Sec. 2.1 was a fourth-order Runge-Kutta integration scheme using double precision arithmetic on IBM 360/65 digital computer system. It was found advantageous to first solve the set of equations given in Eq. (2.1) with appropriate boundary conditions. Using these results, solutions to Eqs. (2.2) and (2.3) were acquired. Finally, the results for Eqs. (2.1) and (2.2) were employed to obtain solutions to Eq. (2.4). The technique for solving each set of equations is now outlined with additional information for solving ordinary differential equations of the boundary layer type available elsewhere [8,9]. Since the integration scheme requires knowledge of values for the functions as well as their derivatives at $\eta = 0$, initial guesses for the unknown derivatives (for example, in Eq. (2.1), $f_1'(0)$ and $S_0'(0)$ are unknown) were made and the integration carried out to some η_{\max} value (initially 2) where boundary conditions specified in Eq. (2.6) must be satisfied. If these boundary conditions were not met, then the guesses for the derivatives must be adjusted and the integration repeated. The method employed to obtain new estimates for the derivatives is attributed to Nachtsheim and Swigert [9]. Upon satisfaction of the boundary conditions for the particular value of η_{\max} , it was then necessary to establish if η_{\max} corresponded to a sufficiently large value as required by Eq. (2.6). η_{\max} was then increased (for example, next value was 4) and the integration scheme as well as adjustment of values for the unknown derivatives repeated until the boundary conditions were

again satisfied. This procedure was continued until values for the unknown derivatives at $\eta = 0$ did not vary. In all cases, the maximum value for η was 8 where all boundary conditions were generally within 10^{-12} of the required values. An integration step size of 0.005 was found to give sufficiently accurate results of at least eight decimal digits for all initial derivatives and reasonable computational times.

A listing of the digital computer program to obtain values of unknown initial derivatives is given in Appendix A. Also, a program which uses these results to generate the values for all functions at different η values for listing, plotting and analysis purposes is supplied. Results from this numerical method are presented in Chapter 4.

4. DISCUSSION OF RESULTS

4.1 Solutions of governing equations

Utilising the method of solution as discussed in Chapter 3, solutions for the unknown values of derivatives at the body surface were acquired for several values of wall enthalpy difference S_w from -1 to 6 and results presented in Table 4.1. Employing these values as well as those in Eq. (2.5) as initial conditions for the Runge-Kutta integration scheme, velocity and temperature functions were evaluated for different values of the similar independent variable and are presented in Figs. 4.1, 4.2, 4.3 and 4.4 for Eqs. (2.1), (2.2), (2.3) and (2.4), respectively. Only first and second derivative results for the velocity functions are displayed since these correspond to velocity and shear stress, respectively. As identified in Sec. 2.2, the various quantities used to describe boundary layer characteristics are expressed in terms of the functions f_1 and S_0 for positions near the stagnation point. These functions are shown in Fig. 4.1. Only results are illustrated for values of η up to 4 where it can be observed in the graphs that the boundary conditions specified by Eq. (2.6) are adequately satisfied. Several general comments can be made concerning results presented in these figures. First, tangential velocities within the boundary layer may exceed the boundary layer edge velocity. This can be observed by recognizing the greater than unity values shown by the first derivatives of the velocity functions. Furthermore, the second derivatives of the velocity functions increase as wall enthalpy difference increases, and the shear stress is expected to exhibit

TABLE 4.1 Surface derivatives for velocity and temperature functions

S_w	$f_1''(0)$	$S_0'(0)$	$g_3''(0)$	$z_2'(0)$	$g_5''(0)$	$z_4'(0)$	$h_5''(0)$	$w_4'(0)$
-1.0	0.82185961	0.69893287	1.7489331	0.72490904	2.0905660	0.93898906	0.57759317	-0.22042164
-0.5	1.0761390	0.36652255	2.4491549	0.39194492	3.1223245	0.52347116	0.67536028	-0.13919842
0.0	1.3119376	0.0	3.0895944	0.0	4.0556969	0.0	0.76999771	0.0
0.5	1.5343082	-0.39377873	3.6888016	-0.43479157	4.9236384	-0.59781512	0.86174012	0.17726846
1.0	1.7462793	-0.81018297	4.2570991	-0.90344018	5.7436466	-1.1252388	0.95079634	0.38234580
2.0	2.1464154	-1.6991555	5.3248052	-1.9212323	7.2788461	-2.6926578	1.1218152	0.85384748
4.0	2.8801426	-3.6528033	7.2726883	-4.1982672	10.069236	-5.9555466	1.4412350	1.9662938
6.0	3.5541453	-5.7865918	9.0559369	-6.7146628	12.617621	-9.5889537	1.7382125	3.2348408

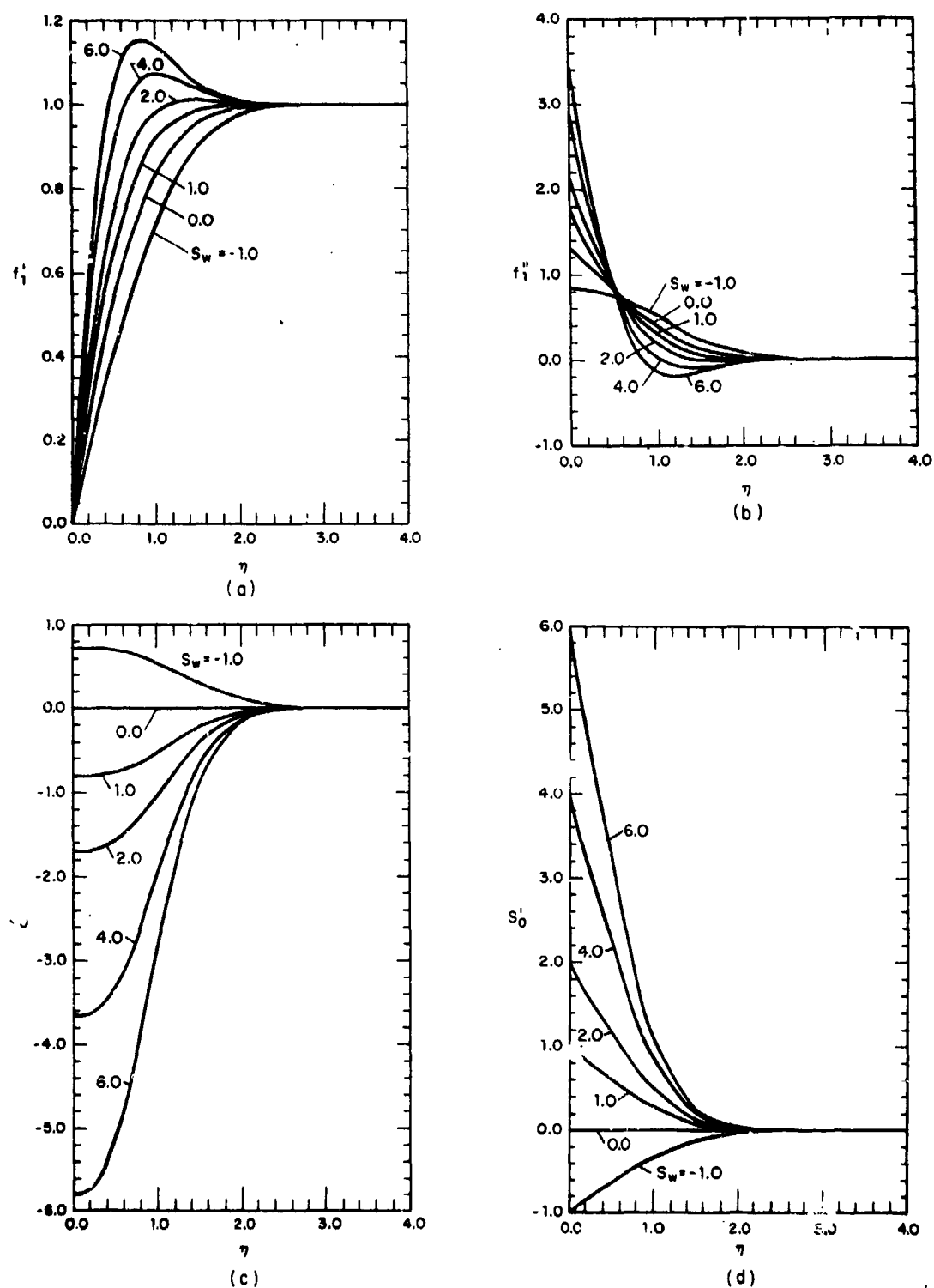


Fig. 4.1 First-order perturbation results

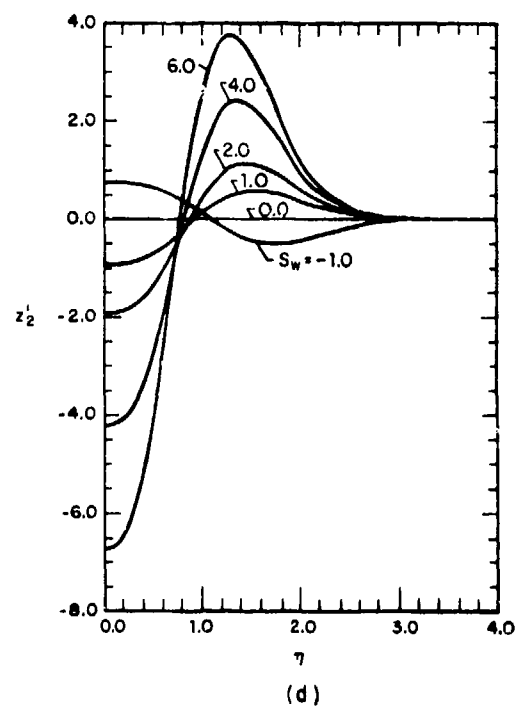
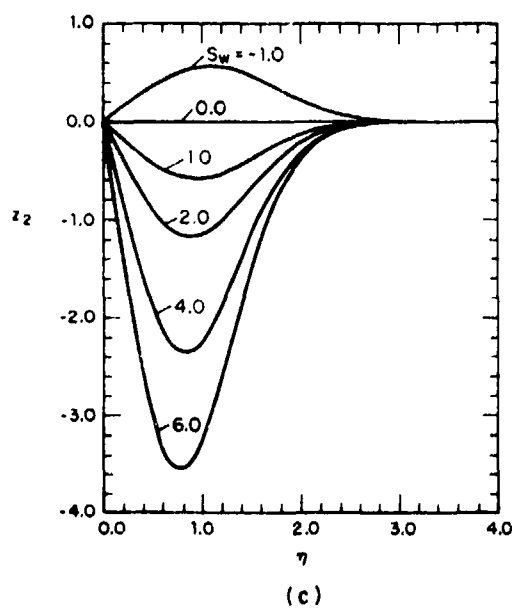
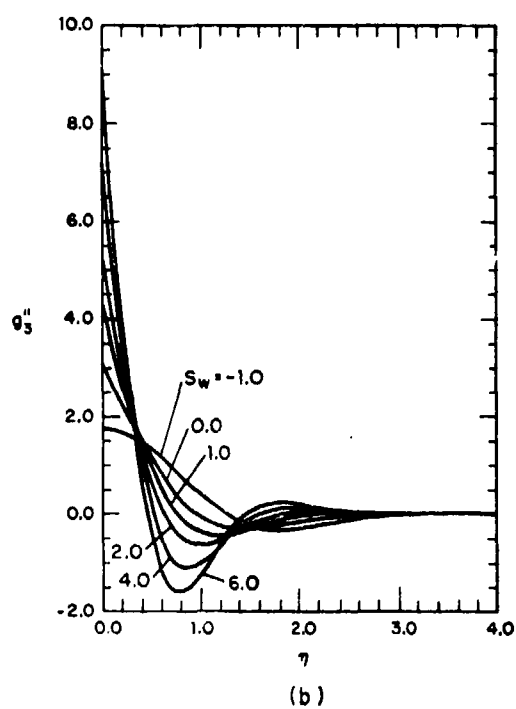
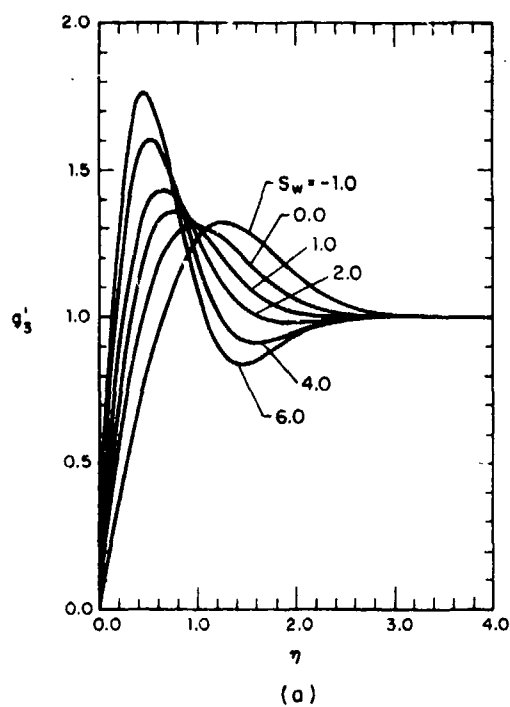


Fig. 4.2 Third-order perturbation results

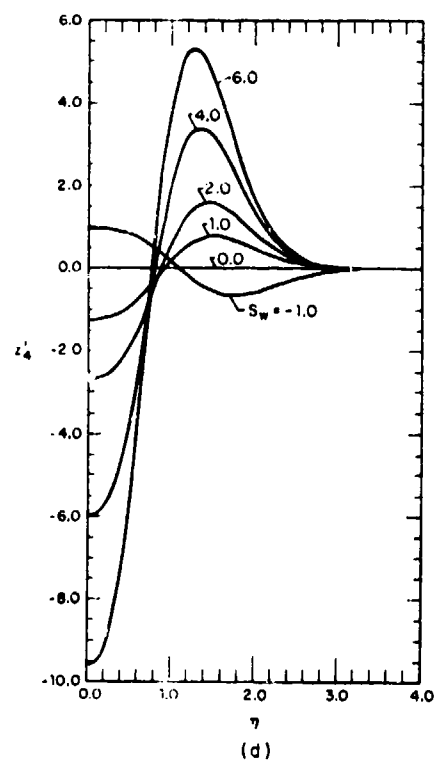
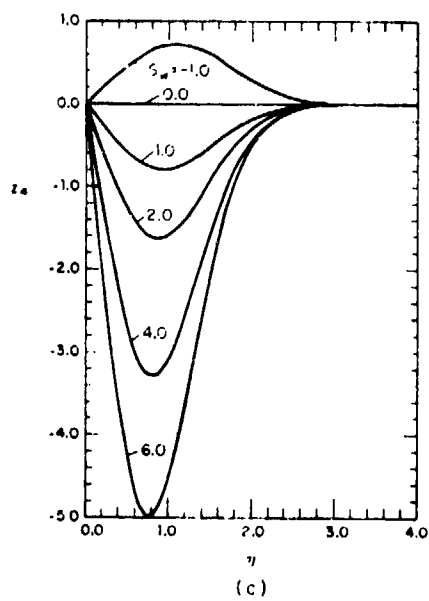
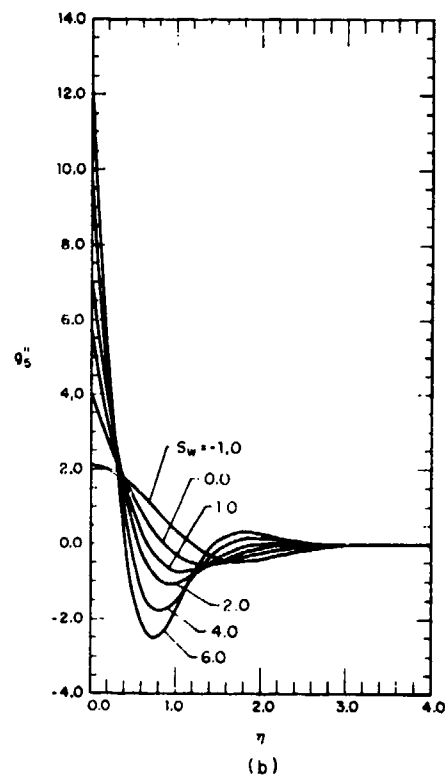
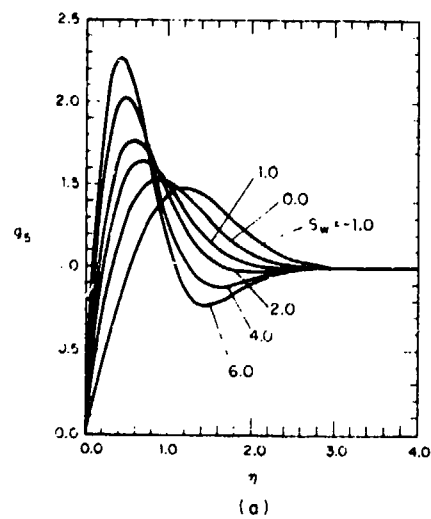


Fig. 4.3 Fifth-order perturbation results, first set of equations

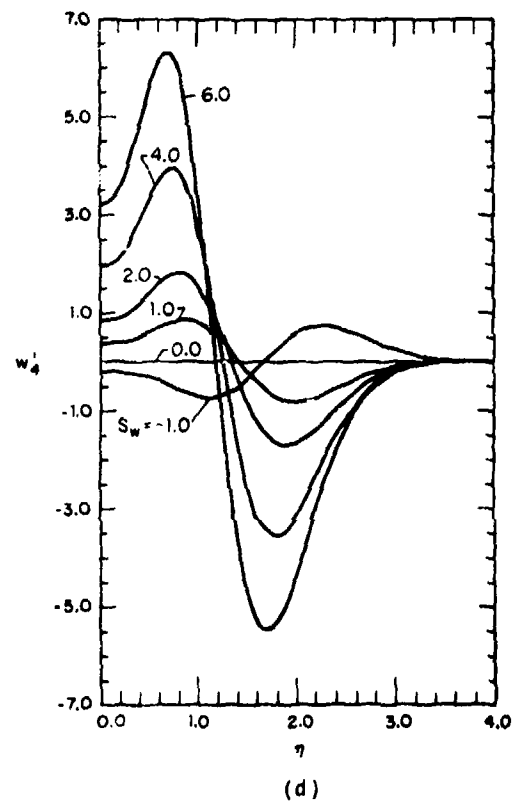
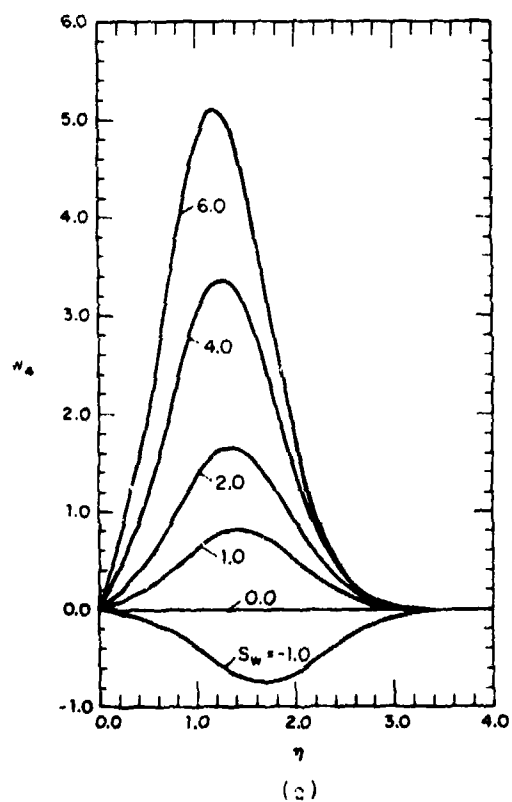
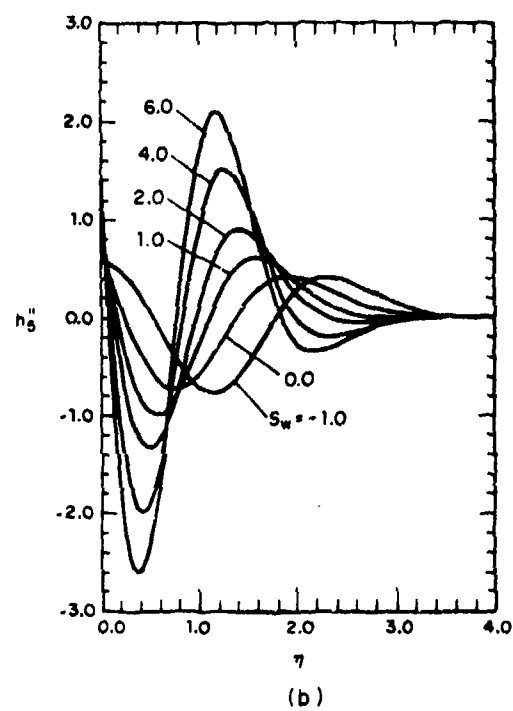
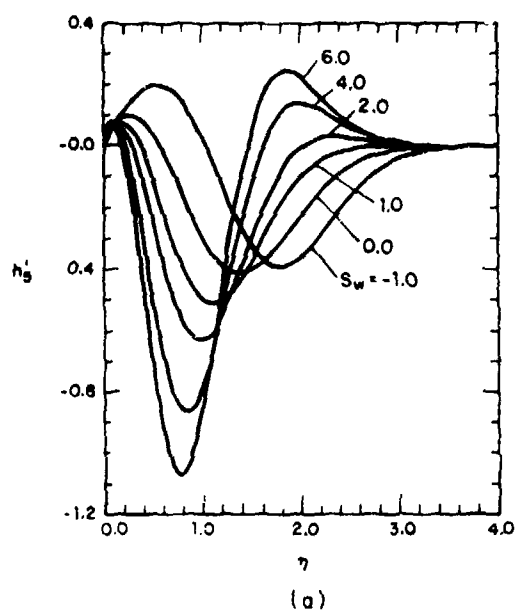


Fig. 4.4 Fifth-order perturbation results, second set of equations

a similar trend. The adiabatic boundary condition yields $S = 0$ throughout the boundary layer. This implies that the total energy ($c_p T_0$) remains constant within the boundary layer and the surface is at the free stream stagnation temperature. Finally, heating of the surface by the gas occurs for wall enthalpy differences less than zero and cooling for wall enthalpy differences greater than zero.

4.2 Results for boundary layer characteristics

Velocity and temperature profiles within the boundary layer for several locations along the body and for various wall enthalpy differences are illustrated in Fig. 4.5 for a Mach number of 1.5 and specific heat ratio of 1.4. Results for $\bar{x} = 0$ correspond to the stagnation region where the boundary layer edge velocity is zero. At this location there would be no hydrodynamic boundary layer. Positions slightly removed from the stagnation point have velocity profiles represented by those for $\bar{x} = 0$ as illustrated by Eq. (2.12b). Tangential velocities greater than the boundary layer velocities are displayed for the higher values of wall enthalpy difference. Velocity ratios greater than unity are attributed to the increase in volume imparted to the gas due to the high wall temperatures. The gas of lower density is accelerated by the pressure in spite of it being decelerated by viscous forces. A thermal boundary exists near the stagnation region for wall temperatures different from the free stream stagnation temperature and grows along the body. The decrease in temperature ratio along the body is a result of an increase in the amount of stagnation energy being transformed into kinetic energy. The

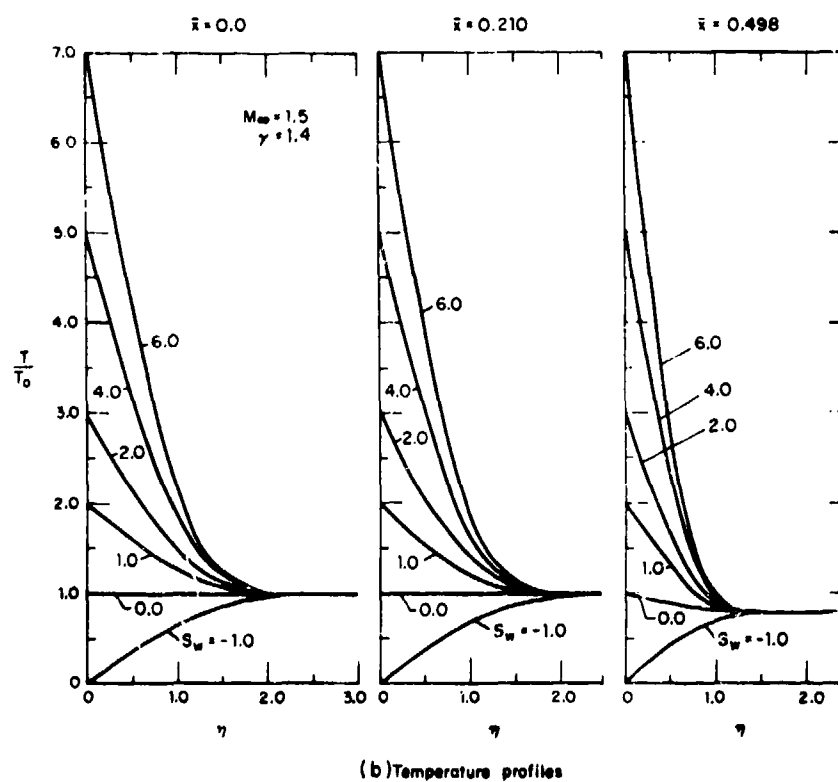
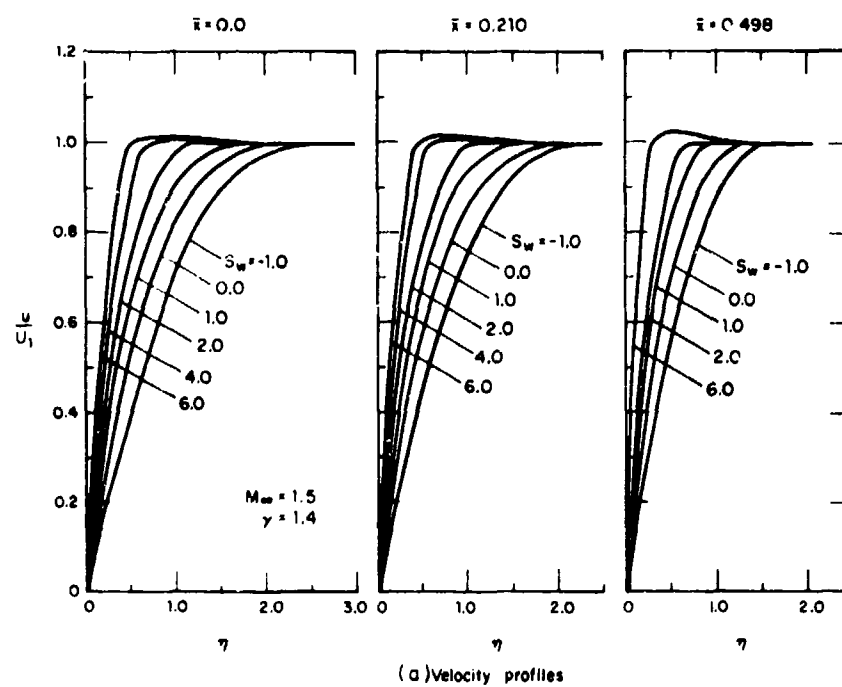


Fig. 4.5 Velocity and temperature profiles ($M_\infty = 1.5$, $\gamma = 1.4$)

boundary layer edge velocity increases from the stagnation point with a corresponding reduction in boundary layer edge temperature. Results for nonuniform wall temperatures can be obtained from those presented in Fig. 4.5 by specifying the wall temperature for each position and selecting the corresponding curve. Boundary layer edge velocity and temperature results are not influenced by the wall temperature.

As previously mentioned, surface shear stress is related to the drag experienced by a body as it passes through a gas. Representative values for shear stress normalized with respect to the factor of $\sqrt{\mu_0 \gamma P_0 \beta}$ are illustrated in Fig. 4.6 as a function of distance along the body for a free stream Mach number of 1.5 and specific heat ratio of 1.4. The maximum distance along the body for which the analysis [3] applies is limited by the applicability of the method to describe the boundary layer edge velocity. Results for a particular value of wall enthalpy difference correspond to an isothermal surface. For nonisothermal surfaces, similar results can be obtained from those presented in Fig. 4.6 provided the distribution of wall enthalpy difference along the body is specified. Results illustrate that wall shear stress is lower when the surface is cooled. This is attributed to wall dynamic viscosity ($\mu_w \sim T_w$) and second derivatives of velocity functions (see Table 4) exhibiting smaller values on a cooled surface. Near the stagnation region, shear stress increases almost linearly with distance as also can be observed from Eq. (2.17b). The shear stress is found not to be a strong function of wall temperature. For example a twofold increase of wall enthalpy difference from 1.0 to 2.0 yields only about a

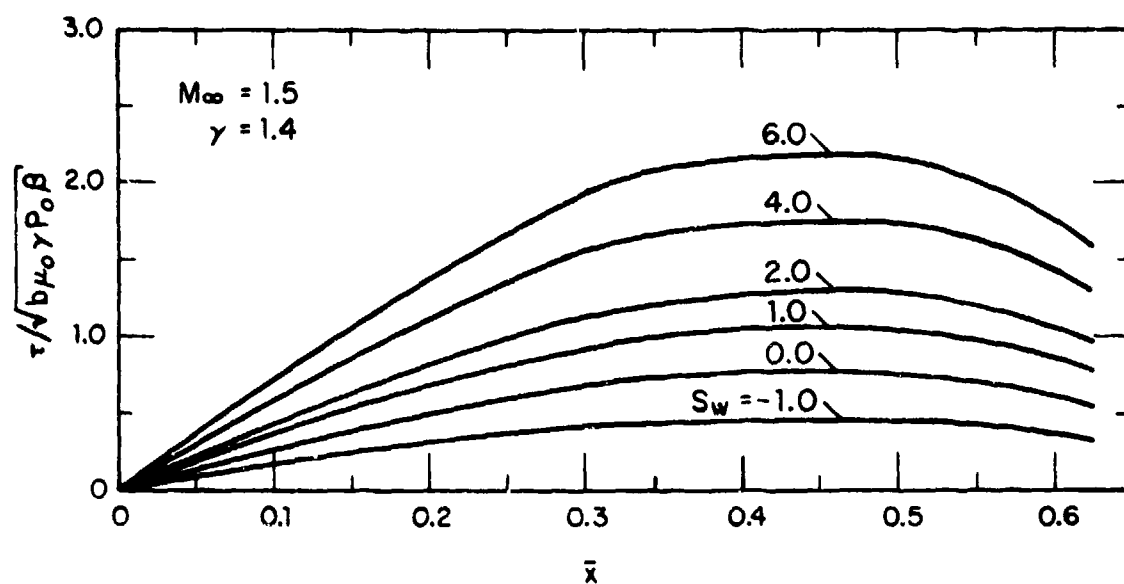


Fig. 4.6 Surface shear stress ($M_\infty = 1.5$, $\gamma = 1.4$)

20% increase in shear stress at a location of 0.4. The decrease in shear stress with increasing distance is believed to be a result of the boundary layer beginning to separate from the body. However, further investigation is needed to establish the validity of this conjecture. Results for the Reynolds number-skin friction parameter as defined in Eq. (2.19a) are displayed in Fig. 4.7 as a function of distance for a Mach number of 1.5 and specific heat ratio of 1.4. Values of this parameter for points near the stagnation region are given by values of $f_1''(0)$ which are tabulated in Table 4.1. This parameter is observed not to be a strong function of distance along the body.

Heat transfer and local Nusselt number results for isothermal surfaces are presented in Fig. 4.8 for several values of wall enthalpy differences with Mach number of 1.5 and specific heat ratio of 1.4. The surface is cooled for values of wall enthalpy difference less than zero and heated for values greater than zero. Results corresponding to zero heat flux are for adiabatic surface where the wall temperature is equal to the free stream stagnation temperature. For $S_w = -1.0$, the wall temperature is at absolute zero and, thus, there would be an infinite heat transfer rate to the surface. Near the stagnation region, heat flux is given by the function $S_0'(0)$ and is nearly independent of distance. A twofold increase of wall enthalpy difference from 1.0 to 2.0 yields approximately 40% increase in heat flux for the stagnation region. The decrease of heat flux with distance is believed to be attributed to boundary layer separation. Evaluation of Nusselt number for adiabatic wall condition poses problems since both S_w and $S'(0)$ are

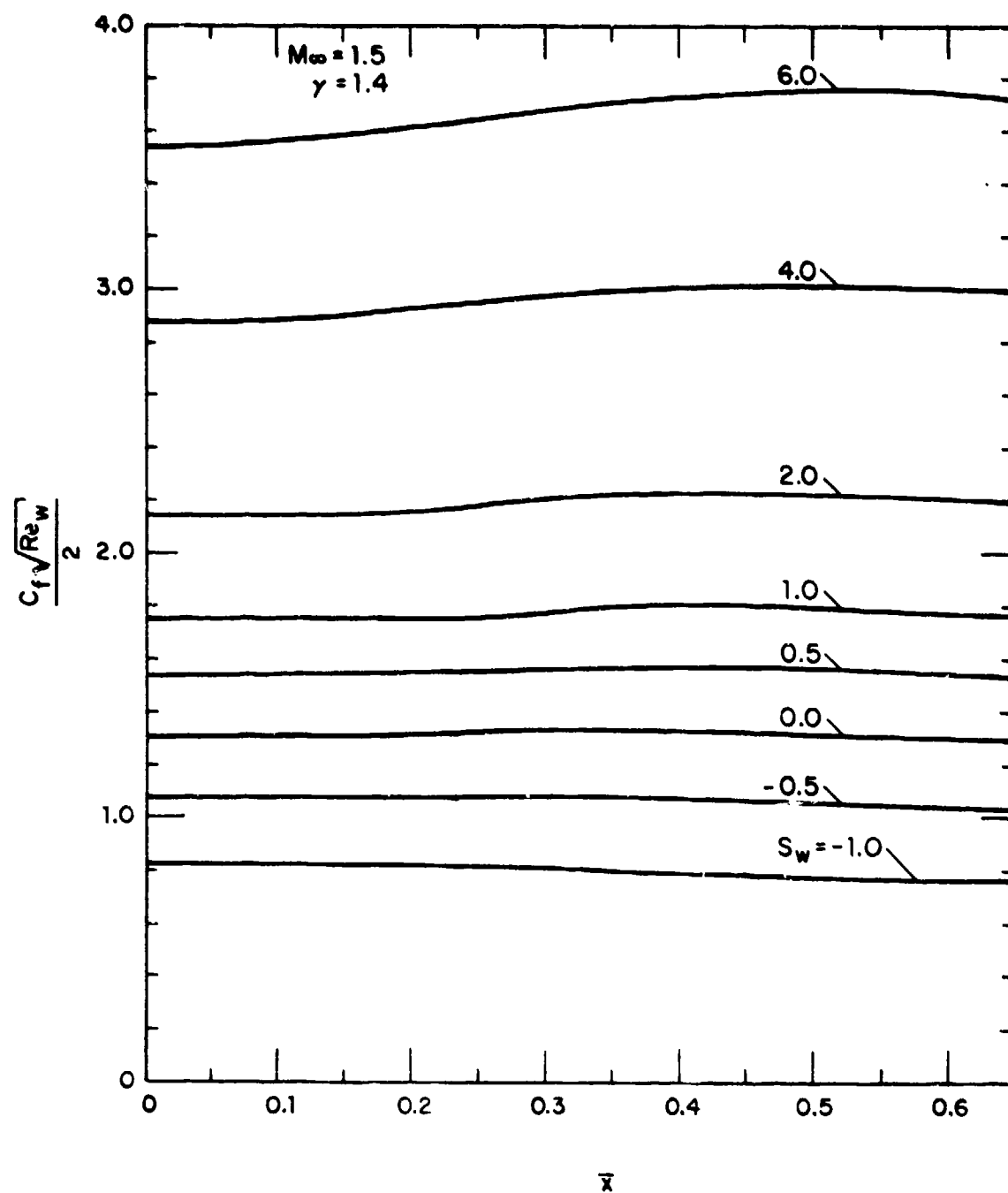
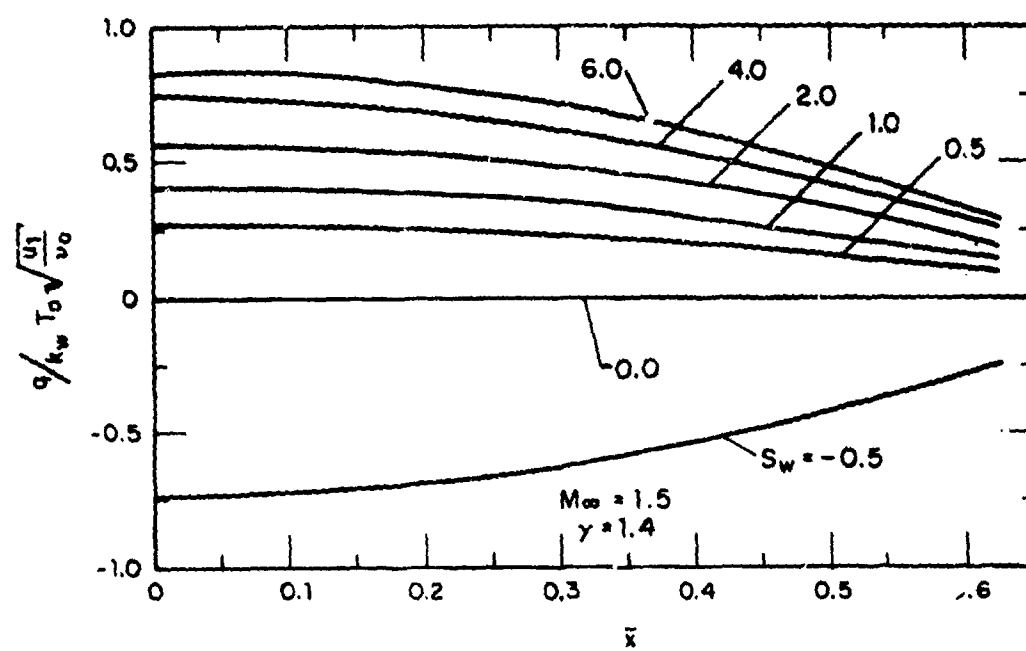
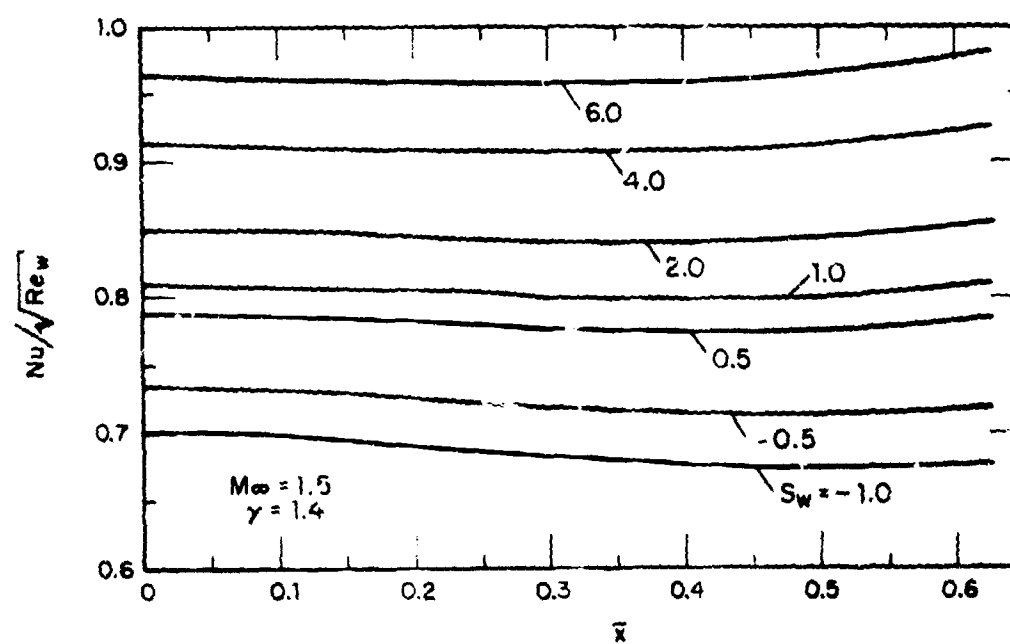


Fig. 4.7 Reynolds number-skin friction parameter
($M_\infty = 1.5$, $\gamma = 1.4$)



(a) Heat transfer



(b) Nusselt number

Fig. 4.8 Heat transfer and Nusselt number
($M_\infty = 1.5$, $\gamma = 1.4$)

zero. However, results from some preliminary numerical experiments illustrate that as S_w approaches zero, the ratio of the first term for $S'(0)$ to S_w , namely, $S'_0(0)/S_w$ approaches a value of about 0.76. Thus, it appears that the Nusselt number is defined for adiabatic wall boundary condition. Additional information is needed to further define this ratio.

The relationship between fluid friction and heat transfer is expressed by the Reynolds analogy parameter which is shown in Fig. 4.9 as a function of distance along the body for several wall enthalpy difference values with Mach number of 1.5 and specific heat ratio of 1.4. Near the stagnation region, this parameter is given by Eq. (2.25b) which includes the ratio of $S_w/S'_0(0)$. For the adiabatic wall condition, this ratio appears to acquire a value of 1.3. This then results in a value of 1.7 for the Reynolds analogy parameter. This parameter exhibits values which are greater than unity and which increase with wall enthalpy difference. These trends are similar to those found in other investigations [7,10].

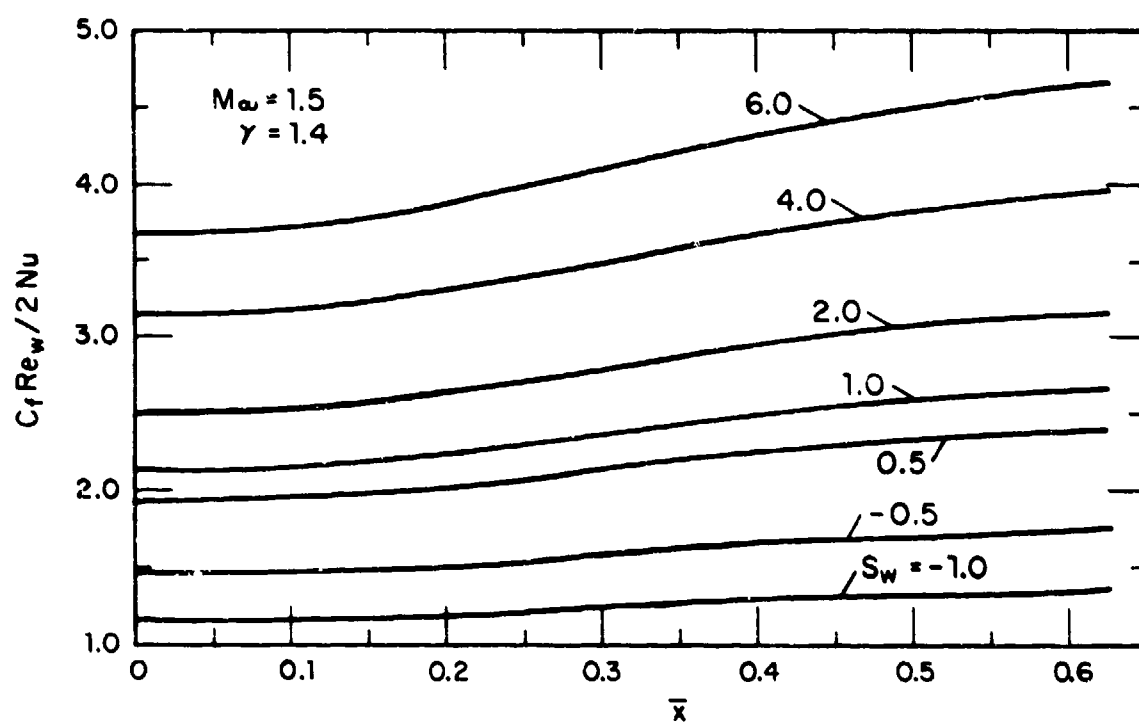


Fig. 4.9 Reynolds analogy parameter ($M_\infty = 1.5$, $\gamma = 1.4$)

5. CONCLUSIONS

An analysis has been developed which transforms the governing transport equations for steady, axisymmetric, compressible, nonrotating boundary layer flow about a body of revolution into a set of nonlinear coupled ordinary differential equations. Solutions to the ordinary differential equations subjected to specified boundary conditions were obtained using a standard numerical integration technique. Results were presented for velocity and temperature profiles within the boundary layer as well as skin friction and heat transfer rates along the body.

Several additional studies are necessary in order to completely establish the applicability of the present analysis. First, the accuracy of including each successive term in the perturbation scheme needs to be examined. Near the stagnation region of the body, the first term would be sufficient. However, the effect of additional terms for points removed from this area needs to be established. Second, additional results from this analysis for other values of the parameters should be acquired and analyzed for trends. There is a need to better define the ratio of $S'(0)/S_w$ as S_w approaches zero. Third, comparison of results from the analysis with experimental results would help to establish the range of applicability of the analysis. Comparison of present results with numerical solutions of the governing transport equations should be considered. Finally, temperatures within the boundary layer may attain sufficient levels where gaseous radiation

can contribute significantly to surface heat flux. Effects of radiant transport within the boundary layer and at the body surface need to be defined.

6. REFERENCES

- [1] "Retrieval of Aerodynamic Heating Information, part 1, Unclassified Materials," NOTS 4137, U. S. Naval Ordnance Test Station, China Lake, California (1967).
- [2] Moore, F. K., "Three-Dimensional Laminar Boundary Flow," JAS 20, 525-534 (1953).
- [3] Chou, D. C., "Aerodynamic Heating of Cannon Launched Guided Projectiles," U. S. Army Contract No. DAHC04-72-A0001 (1974).
- [4] Schlichting, H., Boundary-Layer Theory, 6th edition, McGraw-Hill Book Co., New York (1968).
- [5] Shapiro, A. H., The Dynamics and Thermodynamics of Compressible Fluid Flow, Vol. II, Ronald Press, New York (1954).
- [6] Kreith, F., Principles of Heat Transfer, 3rd edition, Intext, New York (1973).
- [7] Li, T. Y. and Nagamatsu, H. T., "Similar Solutions of Compressible Boundary-Layer Equations," JAS 22, 607-616 (1955).
- [8] Adams, J. A. and Rogers, D. F., Computer-Aided Heat Transfer Analysis, McGraw-Hill, New York (1973).
- [9] Nachtsheim, P. R. and Swigert, P., "Satisfaction of Asymptotic Boundary Conditions in Numerical Solution of Systems of Nonlinear Equations of the Boundary-Layer Type," NASA TN D-3004 (1965).
- [10] Li, T. Y and Nagamastu, H. T., "Similar Solutions of Compressible Boundary-Layer Equations," JAS 20, 653-655 (1953).

APPENDIX A

Computer programs employed to obtain solutions to the ordinary differential equations as well as to obtain lists and plots of these solutions are furnished. For convenience in discussing the programs, Eqs. (2.1), (2.2), (2.3) and (2.4) are referred to by AERO, AER1, AER2 and AER3, respectively. The computer program called AER used to solve for values of the unknown derivatives at $\eta = 0$ includes MAIN, READ, RUNKUT, FCN and INCON routines. The purpose of each routine is briefly noted in Table A-1. The FCN routine is different for each AER. Furthermore, as observed by boundary condition in Eq. (2.6), the routine INCON is slightly different for AER3. Initial values for the functions as well as their derivatives at $\eta = 0$ may be substituted into the AERL program to generate lists or plots. Routines which make-up AERL are briefly described in Table A-2. Listing of routines for AERL is also supplied.

TABLE A-1 Computer Program AER

Routine	Description
MAIN	Controls calling sequence for other routines.
READ	Input of program parameters as well as initial values for known and unknown functions at $\eta = 0$.
RUNKUT	Fourth-order Runge-Kutta integration scheme from $\eta = 0$ to η_{\max} in steps of $\Delta\eta$.
FCN	Evaluates functions at specified value of η . Includes perturbation equations for adjusting guesses [9].
INCON	Adjusts initial values for unknown derivatives and checks for convergence.

MAIN

```

C INTEGRATION OF ORDINARY DIFFERENTIAL EQUATIONS
  IMPLICIT REAL*8(A-H,O-Z)
  DIMENSION F(3,15),FD(3,15)
C READ INPUT VARIABLES
1   CALL READ(NOD,NOR,H,ETAO,ETAM,EMAX,FD,NEQ)
    NADJ=1
C RUNGE-KUTTA INTEGRATION
2   CALL RUNKUT(NOD,NOR,H,ETAO,ETAM,FD,F,NEQ)
C ADJUST INITIAL CONDITIONS
  CALL INCON(ETAM,EMAX,FD,F,NADJ,NEQ,NOD)
  WRITE(6,100) NADJ
  IF(NADJ.NE.0) GO TO 2
  GO TO 1
100  FORMAT(10X,'INITIAL CONDITION',I5)
    END

```

READ

```

SUBROUTINE READ(NOD,NOR,H,ETAO,ETAM,EMAX,FD,NEQ)
C INPUT PARAMETERS
  IMPLICIT REAL*8(A-H,O-Z)
  DIMENSION FD(3,15),TITLE(10)
C*****
C NOD   NUMBER OF FUNCTIONS AND DERIVATIVES
C NOR   NUMBER OF DESIRED FUNCTIONS AND DERIVATIVES
C NEO   NUMBER OF EQUATION SETS
C H     INTERVAL SIZE FOR ETA
C ETAO  INITIAL VALUE FOR ETA
C ETAM  INITIAL VALUE FOR MAXIMUM ETA
C EMAX  MAXIMUM ETA
C FD     INITIAL BOUNDARY CONDITIONS AT ETA=ETAO
C*****
C READ IN TITLE CARD
  READ(5,102,END=99) TITLE
C READ IN PROGRAM PARAMETERS
  READ(5,100) NOD,NOR,NEQ,H,ETAO,ETAM,EMAX
C READ IN INITIAL VALUES OF FUNCTIONS AND THEIR DERIVATIVES
  READ(5,101)((FD(I,J),J=1,NOD),I=1,NEQ)
C PRINT OUT INPUTS
  WRITE(6,103) TITLE,FD(1,4),H
  WRITE(6,101)((FD(I,J),J=1,NOD),I=1,NEQ)
  RETURN
99  CALL EXIT
100  FORMAT(3I5,4D15.7)
101  FORMAT(3D25.16)
102  FORMAT(10A8)
103  FORMAT(14I,10A8///17X,'SW=',D15.7//
110X,'STEP SIZE=',F6.4//10X,'INITIAL CONDITIONS')
  END

```

RUNKUT

```

SUBROUTINE RUNKUT(NOD,NOR,H,ETA0,ETAM,FD,F,NEQ)
C RUNGE KUTTA INTEGRATION SCHEME
  IMPLICIT REAL*8(A-H,O-Z)
  DIMENSION FD(3,15),F(3,15),FC(3,15),AK1(3,15),AK2(3,15),
1 AK3(3,15),AK4(3,15)
C ZERO ARRAYS
  DO 7 I=1,NEQ
    DO 7 J=1,NOD
      F(I,J)=0.00
      FC(I,J)=0.00
      FD(I,J)=0.00
      AK1(I,J)=0.00
      AK2(I,J)=0.00
      AK3(I,J)=0.00
7    AK4(I,J)=0.00
C INITIAL CONDITIONS
  IE=1
  DO 1 J=1,NEQ
    DO 1 I=1,NOD
      F(J,I)=F(J,I)
1    FC(J,I)=FC(J,I)
      WRITE(6,101)
      WRITE(6,100) ETA0,(F(NEQ,I),I=1,NOR)
      CALL FCN(ETA0,FC,FD)
C INTEGRATION
2    ETA=ETA0+(IE-1)*H
      DO 3 J=1,NEQ
        DO 3 I=1,NOD
          AK1(J,I)=H*FD(J,I)
3      FC(J,I)=F(J,I)+0.500*AK1(J,I)
      ETA=ETA+0.500*H
      CALL FCN(ETA,FC,FD)
      DO 4 J=1,NEQ
        DO 4 I=1,NOD
          AK2(J,I)=H*FD(J,I)
4      FC(J,I)=F(J,I)+0.500*AK2(J,I)
      CALL FCN(ETA,FC,FD)
      DO 5 J=1,NEQ
        DO 5 I=1,NOD
          AK3(J,I)=H*FD(J,I)
5      FC(J,I)=F(J,I)+AK3(J,I)
      ETA=ETA+0.500*H
      CALL FCN(ETA,FC,FD)
      DO 6 J=1,NEQ
        DO 6 I=1,NOD
          AK4(J,I)=H*FD(J,I)
6      F(J,I)=F(J,I)+(AK1(J,I)+2.00*(AK2(J,I)+AK3(J,I))+AK4(J,I))/6.00
      IE=IE+1
      IF(ETA.LT.ETAM) GO TO 2
      WRITE(6,100) ETA,(F(NEQ,I),I=1,NOR)
      RETURN
100  FORMAT(F7.2,5D25.16)
101  FORMAT(/3X,'ETA',12X,'F',24X,'F*',23X,'F**',24X,'G',23X,'G*')
END

```

FCN FOR AERO

```

SUBROUTINE FCN(ETA,F,FD)
C FUNCTIONS FOR AERO
  IMPLICIT REAL*8(A-H,O-Z)
  DIMENSION F(3,15),FD(3,15)
C DIFFERENTIAL EQUATIONS
  FD(1,1)=F(1,2)
  FD(1,2)=F(1,3)
  FD(1,3)=-2.00*F(1,1)*F(1,3)+F(1,2)*F(1,2)-F(1,4)-1.00
  FD(1,4)=F(1,5)
  FD(1,5)=-2.00*F(1,1)*F(1,5)
C X PERTURBATION
  FD(1,6)=F(1,7)
  FD(1,7)=F(1,8)
  FD(1,8)=-2.00*(F(1,6)*F(1,3)+F(1,1)*F(1,8))+2.00*F(1,2)*F(1,7)
  1-F(1,9)
  FD(1,9)=F(1,10)
  FD(1,10)=-2.00*(F(1,6)*F(1,5)+F(1,1)*F(1,10))
C Y PERTURBATION
  FD(1,11)=F(1,12)
  FD(1,12)=F(1,13)
  FD(1,13)=-2.00*(F(1,11)*F(1,3)+F(1,1)*F(1,13))+2.00*F(1,2)*F(1,12)
  1-F(1,14)
  FD(1,14)=F(1,15)
  FD(1,15)=-2.00*(F(1,11)*F(1,5)+F(1,1)*F(1,15))
  RETURN
  END

```

FCN FOR AER1

```

SUBROUTINE FCN(ETA,F,FD)
IMPLICIT REAL*8(A-Z)
DIMENSION F(3,15),FD(3,15)
C AERO EQUATIONS
FD(1,1)=F(1,2)
FD(1,2)=F(1,3)
FD(1,3)=-2.00*F(1,1)*F(1,3)+F(1,2)*F(1,2)-F(1,4)-1.00
FD(1,4)=F(1,5)
FD(1,5)=-2.00*F(1,1)*F(1,5)
C AER1 EQUATIONS
C DIFFERENTIAL EQUATIONS
FD(2,1)=F(2,2)
FD(2,2)=F(2,3)
FD(2,3)=-2.00*F(1,1)*F(2,3)+4.00*F(1,2)*F(2,2)-4.00*F(1,3)*
1F(2,1)-2.00*F(1,1)*F(1,3)-4.00*(1.00+F(1,4))-F(2,4)
FD(2,4)=F(2,5)
FD(2,5)=-2.00*F(1,1)*F(2,5)+2.00*F(1,2)*F(2,4)-4.00*F(2,1)*
2F(1,5)-2.00*F(1,1)*F(1,5)
C X-PERTURBATION
FD(2,6)=F(2,7)
FD(2,7)=F(2,8)
FD(2,8)=-2.00*F(1,1)*F(2,8)+4.00*F(1,2)*F(2,7)-4.00*F(1,3)*
3F(2,6)-F(2,9)
FD(2,9)=F(2,10)
FD(2,10)=-2.00*F(1,1)*F(2,10)+2.00*F(1,2)*F(2,9)-4.00*F(1,5)*
4F(2,6)
C Y-PERTURBATION
FD(2,11)=F(2,12)
FD(2,12)=F(2,13)
FD(2,13)=-2.00*F(1,1)*F(2,13)+4.00*F(1,2)*F(2,12)-4.00*F(1,3)*
5F(2,11)-F(2,14)
FD(2,14)=F(2,15)
FD(2,15)=-2.00*F(1,1)*F(2,15)+2.00*F(1,2)*F(2,14)-4.00*F(1,5)*
6F(2,11)
RETURN
END

```


FCN FOR AER2

```

SUBROUTINE FCN(ETA,F,FD)
IMPLICIT REAL*8(A-H,O-Z)
DIMENSION F(3,15),FD(3,15)
C AERO EQUATIONS
FD(1,1)=F(1,2)
FD(1,2)=F(1,3)
FD(1,3)=-2.00*F(1,1)*F(1,3)+F(1,2)*F(1,2)-F(1,4)-1.00
FD(1,4)=F(1,5)
FD(1,5)=-2.00*F(1,1)*F(1,5)
C AER2 EQUATIONS.
C DIFFERENTIAL EQUATIONS
FD(2,1)=F(2,2)
FD(2,2)=F(2,3)
FD(2,3)=-2.00*F(1,1)*F(2,3)+6.00*F(1,2)*F(2,2)-6.00*F(1,3)*F(2,1)
1-4.00*F(1,1)*F(1,3)-6.00*(1.00+F(1,4))-F(2,4)
FD(2,4)=F(2,5)
FD(2,5)=-2.00*F(1,1)*F(2,5)+4.00*F(1,2)*F(2,4)-6.00*F(1,5)*F(2,1)
2-4.00*F(1,1)*F(1,5)
C X-PERTURBATION
FD(2,6)=F(2,7)
FD(2,7)=F(2,8)
FD(2,8)=-2.00*F(1,1)*F(2,8)+6.00*F(1,2)*F(2,7)-6.00*F(1,3)*F(2,6)
7-F(2,9)
FD(2,9)=F(2,10)
FD(2,10)=-2.00*F(1,1)*F(2,10)+4.00*F(1,2)*F(2,9)-6.00*F(1,5)*
3F(2,6)
C Y-PERTURBATION
FD(2,11)=F(2,12)
FD(2,12)=F(2,13)
FD(2,13)=-2.00*F(1,1)*F(2,13)+6.00*F(1,2)*F(2,12)-6.00*F(1,3)*
5F(2,11)-F(2,14)
FD(2,14)=F(2,15)
FD(2,15)=-2.00*F(1,1)*F(2,15)+4.00*F(1,2)*F(2,14)-6.00*F(1,5)*
1F(2,11)
RETURN
END

```

FCN FOR AER3

```

SUBROUTINE FCN(ETA,F,FD)
IMPLICIT REAL*8(A-H,O-Z)
DIMENSION F(3,15),FD(3,15)
C AERO EQUATIONS
FD(1,1)=F(1,2)
FD(1,2)=F(1,3)
FD(1,3)=-2.00*F(1,1)*F(1,3)+F(1,2)*F(1,2)-F(1,4)-1.00
FD(1,4)=F(1,5)
FD(1,5)=-2.00*F(1,1)*F(1,5)
C AER1 EQUATIONS
FD(2,1)=F(2,2)
FD(2,2)=F(2,3)
FD(2,3)=-2.00*F(1,1)*F(2,3)+4.00*F(1,2)*F(2,2)-4.00*F(1,3)*
1F(2,1)-2.00*F(1,1)*F(1,3)-4.00*(1.00+F(1,4))-F(2,4)
FD(2,4)=F(2,5)
FD(2,5)=-2.00*F(1,1)*F(2,5)+2.00*F(1,2)*F(2,4)-4.00*F(2,1)*
2F(1,5)-2.00*F(1,1)*F(1,5)
C AER3 EQUATIONS
C DIFFERENTIAL EQUATIONS
FD(3,1)=F(3,2)
FD(3,2)=F(3,3)
FD(3,3)=-2.00*F(1,1)*F(3,3)+6.00*F(1,2)*F(3,2)-6.00*F(1,3)*
1F(3,1)-F(3,4)+3.00*F(2,2)*F(2,2)-4.00*F(2,1)*F(2,3)-2.00*F(1,3)
2F(2,1)-2.00*F(1,1)*F(2,3)-3.00*(1.00+F(1,4))+2.00*F(1,1)*
3F(1,3)-4.00*F(2,4)
FD(3,4)=F(3,5)
FD(3,5)=-2.00*F(1,1)*F(3,5)+4.00*F(1,2)*F(3,4)+2.00*F(2,2)*
1F(2,4)-4.00*F(2,1)*F(2,5)-2.00*F(1,1)*F(2,5)-6.00*F(1,5)*
2F(3,1)-2.00*F(1,5)*F(2,1)+2.00*F(1,1)*F(1,5)
C X-PERTURBATION
FD(3,6)=F(3,7)
FD(3,7)=F(3,8)
FD(3,8)=-2.00*F(1,1)*F(3,8)+6.00*F(1,2)*F(3,7)-6.00*F(1,3)*
1F(3,6)-F(3,9)
FD(3,9)=F(3,10)
FD(3,10)=-2.00*F(1,1)*F(3,10)+4.00*F(1,2)*F(3,9)-6.00*F(1,5)*
1F(3,6)
C Y-PERTURBATION
FD(3,11)=F(3,12)
FD(3,12)=F(3,13)
FD(3,13)=-2.00*F(1,1)*F(3,13)+6.00*F(1,2)*F(3,12)-6.00*F(1,3)*
1F(3,11)-F(3,14)
FD(3,14)=F(3,15)
FD(3,15)=-2.00*F(1,1)*F(3,15)+4.00*F(1,2)*F(3,14)-6.00*F(1,5)*
1F(3,11)
RETURN
END

```

INCON FOR AERO, AER1 AND AER2

```

SUBROUTINE INCON(ETAM,EMAX,FOF,FF,NADJ,NEQ,NOD)
C ADJUST INITIAL CONDITIONS
IMPLICIT REAL*8(A-H,O-Z)
DIMENSION FO(15),F(15),FOF(3,15),FF(3,15)
DO I=1,NOD
  FO(I)=FOF(NEQ,I)
  F(I)=FF(NEQ,I)
  A11=F(7)*F(7)+F(9)*F(9)+F(8)*F(8)+F(10)*F(10)
  A12=F(7)*F(12)+F(9)*F(14)+F(8)*F(13)+F(10)*F(15)
  A21=A12
  A22=F(12)*F(12)+F(14)*F(14)+F(13)*F(13)+F(15)*F(15)
  B1=-((F(2)-1.00)*F(7)+F(4)*F(9)+F(3)*F(8)+F(5)*F(10))
  B2=-((F(2)-1.00)*F(12)+F(4)*F(14)+F(3)*F(13)+F(5)*F(15))
  DEY=A11+A22-A12*A21
  DEX=(A22*B1-A12*B2)/DEN
  DEY=(A11*B2-A21*B1)/DEN
  FO(3)=FO(3)+DEX
  FO(5)=FO(5)+DEY
  FOF(NEQ,3)=FO(3)
  FOF(NEQ,5)=FO(5)
C CONVERGENCE CHECKS
  WRITE(6,100) DEX,DEY
  IF(DABS(DEX/FO(3)).GT..1D-12.OR.DABS(DEY/FO(5)).GT..1D-12) RETURN
  E=(F(2)-1.00)**2+F(4)*F(4)+F(3)*F(3)+F(5)*F(5)
  WRITE(6,101) E
  ETAM=2.00*ETAM
  WRITE(6,102) ETAM
  IF(ETAM.LE.EMAX) RETURN
  ETAM=EMAX
  NADJ=NADJ+1
  RETURN
100  FORMAT(10X,'CHECK DEX AND DEY',2D15.7)
101  FORMAT(10X,'CHECK E',10X,D15.7)
102  FORMAT(10X,'CHECK ETAM',7X,D15.7)
END

```

INCON FOR AER3

```

SUBROUTINE INCON(ETAM,EMAX,FOF,FF,NADJ,NEQ,NOD)
C ADJUST INITIAL CONDITIONS
IMPLICIT REAL*8(A-H,O-Z)
DIMENSION FO(15),F(15),FOF(3,15),FF(3,15)
DO 1 I=1,NOD
FO(I)=FOF(NEQ,I)
1 F(I)=FF(NEQ,I)
A11=F(7)*F(7)+F(9)*F(9)+F(8)*F(8)+F(10)*F(10)
A12=F(7)*F(12)+F(9)*F(14)+F(8)*F(13)+F(10)*F(15)
A21=A12
A22=F(12)*F(12)+F(14)*F(14)+F(13)*F(13)+F(15)*F(15)
B1=-(F(2)*F(7)+F(4)*F(9)+F(3)*F(8)+F(5)*F(10))
B2=-(F(2)*F(12)+F(4)*F(14)+F(3)*F(13)+F(5)*F(15))
DEN=A11*A22-A12*A21
DEX=(A22*B1-A12*B2)/DEN
DEY=(A11*B2-A21*B1)/DEN
FO(3)=FO(3)+DEX
FO(5)=FO(5)+DEY
FOF(NEQ,3)=FO(3)
FOF(NEQ,5)=FO(5)
C CONVERGENCE CHECKS
WRITE(6,100) DEX,DEY
IF(DABS(DEX/FO(3)).GT..1D-12.OR.DABS(DEY/FO(5)).GT..1D-12) RETURN
E=F(2)*F(2)+F(4)*F(4)+F(3)*F(3)+F(5)*F(5)
WRITE(6,101) E
ETAM=2.DD*ETAM
WRITE(6,102) ETAM
IF(ETAM.LE.EMAX) RETURN
ETAM=EMAX
NADJ=0
RETURN
100 FORMAT(10X,'CHECK DEX AND DEY',2D15.7)
101 FORMAT(10X,'CHECK E',10X,D15.7)
102 FORMAT(10X,'CHECK ETAM',7X,D15.7)
END

```

TABLE A-2 Computer Program AERL

Routine	Description
MAIN	Input of program parameters and boundary conditions at $\eta = 0$ for all functions and their derivatives. Lists results and controls all routines.
RUNKUT	Fourth-order Runge-Kutta integration scheme.
FCN	Evaluates functions at specified η

MAIN

```

C LIST OF AER
  IMPLICIT REAL*8(A-H,O-Z)
  COMMON/DATA/G(5,1610)
  DIMENSION F(3,5),FO(3,5),TITLE(10)
C READ IN INITIAL VALUES
1  READ(5,100,END=99) TITLE
   READ(5,101) NOR,NEQ,NPR,H,ETAO,ETAM
   READ(5,102)((FO(I,J),J=1,NOR),I=1,NEQ)
C RUNGE-KUTTA INTEGRATION
  CALL RUNKUT(NOR,NOR,H,ETAO,ETAM,FO,F,NEQ)
C PRINT OUT RESULTS
  NDATA=(ETAM-ETAO)/H+2.001D0
  IPR=1
  WRITE(6,103) TITLE
  DO2 I=1,NDATA
    IF(I.NE.IPR) GO TO 2
    IPR=IPR+NPR
    ETA=ETAO+H*(I-1)
    WRITE(6,104) ETA,(G(J,I),J=1,NOR)
2  CONTINUE
   GO TO 1
99  CALL EXIT
100  FORMAT(10A8)
101  FORMAT(3I5,3D15.7)
102  FORMAT(3D25.16)
103  FORMAT(14I,10A8/3X,'ETA',8X,'F',14X,'F*',11X,'F**',13X,'G',14X,
1'G*')
104  FORMAT(F7.2,5D15.7)
END

```

RUNKUT

```

SUBROUTINE RUNKUT(NDD,NOR,H,ETA0,ETAM,FO,F,NEQ)
C RUNGE KUTTA INTEGRATION SCHEME
  IMPLICIT REAL*8(A-Z)
  COMMON/DATA/G(5,1610)
  DIMENSION FO(3,15),F(3,15),FD(3,15),FC(3,15),AK1(3,15),AK2(3,15),
1 AK3(3,15),AK4(3,15)
C ZERO ARRAYS
  DO 7 I=1,NEQ
    DO 7 J=1,NDD
      F(I,J)=0.00
      FC(I,J)=0.00
      FD(I,J)=0.00
      AK1(I,J)=0.00
      AK2(I,J)=0.00
      AK3(I,J)=0.00
7    AK4(I,J)=0.00
C INITIAL CONDITIONS
  IE=1
  DO 1 J=1,NEQ
    DO 1 I=1,NDD
      F(J,I)=F(J,I)
1    FC(J,I)=FO(J,I)
  DO 8 I=1,NOR
    G(I,IE)=F(NEQ,I)
    CALL FCN(ETA0,FC,FD)
C INTEGRATION
  2    ETA=ETA0+(IE-1)*H
    DO 3 J=1,NEQ
      DO 3 I=1,NDD
        AK1(J,I)=H*FD(J,I)
3      FC(J,I)=F(J,I)+0.500*AK1(J,I)
      ETA=ETA+0.500*H
      CALL FCN(ETA,FC,FD)
      DO 4 J=1,NEQ
        DO 4 I=1,NDD
          AK2(J,I)=H*FD(J,I)
4      FC(J,I)=F(J,I)+0.500*AK2(J,I)
      CALL FCN(ETA,FC,FD)
      DO 5 J=1,NEQ
        DO 5 I=1,NDD
          AK3(J,I)=H*FD(J,I)
5      FC(J,I)=F(J,I)+AK3(J,I)
      ETA=ETA+0.500*H
      CALL FCN(ETA,FC,FD)
      DO 6 J=1,NEQ
        DO 6 I=1,NDD
          AK4(J,I)=H*FD(J,I)
6      F(J,I)=F(J,I)+(AK1(J,I)+2.00*(AK2(J,I)+AK3(J,I))+AK4(J,I))/6.00
      IE=IE+1
      DO 9 I=1,NOR
        G(I,IE)=F(NEQ,I)
9      IF(ETA.LT.ETAM) GO TO 2
      RETURN
      END

```

FCN FOR AERO

```

SUBROUTINE FCN(ETA,F,FD)
C FUNCTIONS FOR AERO
  IMPLICIT REAL*8(A-H,O-Z)
  DIMENSION F(3,15),FD(3,15)
  FD(1,1)=F(1,2)
  FD(2,2)=F(1,3)
  FD(1,3)=-2.00*F(1,1)*F(1,3)+F(1,2)*F(1,2)-F(1,4)-1.00
  FD(1,4)=F(1,5)
  FD(1,5)=-2.00*F(1,1)*F(1,5)
  RETURN
END

```

FCN FOR AER1

```

SUBROUTINE FCN(ETA,F,FD)
  IMPLICIT REAL*8(A-H,O-Z)
  DIMENSION F(3,15),FD(3,15)
C AERO EQUATIONS
  FD(1,1)=F(1,2)
  FD(1,2)=F(1,3)
  FD(1,3)=-2.00*F(1,1)*F(1,3)+F(1,2)*F(1,2)-F(1,4)-1.00
  FD(1,4)=F(1,5)
  FD(1,5)=-2.00*F(1,1)*F(1,5)
C AER1 EQUATIONS
  FD(2,1)=F(2,2)
  FD(2,2)=F(2,3)
  FD(2,3)=-2.00*F(1,1)*F(2,3)+4.00*F(1,2)*F(2,2)-4.00*F(1,3)*
1F(2,1)-2.00*F(1,1)*F(1,3)-4.00*(1.00+F(1,4))-F(2,4)
  FD(2,4)=F(2,5)
  FD(2,5)=-2.00*F(1,1)*F(2,5)+2.00*F(1,2)*F(2,4)-4.00*F(2,1)*
2F(1,5)-2.00*F(1,1)*F(1,5)
  RETURN
END

```


FCN FOR AER2

```

SUBROUTINE FCN(ETA,F,FD)
IMPLICIT REAL*8(A-H,O-Z)
DIMENSION F(3,15),FD(3,15)
C AERO EQUATIONS
FD(1,1)=F(1,2)
FD(1,2)=F(1,3)
FD(1,3)=-2.00*F(1,1)*F(1,3)+F(1,2)*F(1,2)-F(1,4)-1.00
FD(1,4)=F(1,5)
FD(1,5)=-2.00*F(1,1)*F(1,5)
C AER2 EQUATIONS.
FD(2,1)=F(2,2)
FD(2,2)=F(2,3)
FD(2,3)=-2.00*F(1,1)*F(2,3)+6.00*F(1,2)*F(2,2)-6.00*F(1,3)*F(2,1)
1-4.00*F(1,1)*F(1,3)-6.00*(1.00+F(1,4))-F(2,4)
FD(2,4)=F(2,5)
FD(2,5)=-2.00*F(1,1)*F(2,5)+4.00*F(1,2)*F(2,4)-6.00*F(1,5)*F(2,1)
2-4.00*F(1,1)*F(1,5)
RETURN
END

```

FCN FOR AER3

```

SUBROUTINE FCN(ETA,F,FD)
IMPLICIT REAL*8(A-H,O-Z)
DIMENSION F(3,15),FD(3,15)
C AERO EQUATIONS
FD(1,1)=F(1,2)
FD(1,2)=F(1,3)
FD(1,3)=-2.00*F(1,1)*F(1,3)+F(1,2)*F(1,2)-F(1,4)-1.00
FD(1,4)=F(1,5)
FD(1,5)=-2.00*F(1,1)*F(1,5)
C AER1 EQUATIONS
FD(2,1)=F(2,2)
FD(2,2)=F(2,3)
FD(2,3)=-2.00*F(1,1)*F(2,3)+4.00*F(1,2)*F(2,2)-4.00*F(1,3)*
1F(2,1)-2.00*F(1,1)*F(1,3)-4.00*(1.00+F(1,4))-F(2,4)
FD(2,4)=F(2,5)
FD(2,5)=-2.00*F(1,1)*F(2,5)+2.00*F(1,2)*F(2,4)-4.00*F(2,1)*
2F(1,5)-2.00*F(1,1)*F(1,5)
C AER3 EQUATIONS
FD(3,1)=F(3,2)
FD(3,2)=F(3,3)
FD(3,3)=-2.00*F(1,1)*F(3,3)+6.00*F(1,2)*F(3,2)-6.00*F(1,3)*
1F(3,1)-F(3,4)+3.00*F(2,2)*F(2,2)-4.00*F(2,1)*F(2,3)-2.00*F(1,3)
2*F(2,1)-2.00*F(1,1)*F(2,3)-3.00*(1.00+F(1,4))+2.00*F(1,1)*
3F(1,3)-4.00*F(2,4)
FD(3,4)=F(3,5)
FD(3,5)=-2.00*F(1,1)*F(3,5)+4.00*F(1,2)*F(3,4)+2.00*F(2,2)*
1F(2,4)-4.00*F(2,1)*F(2,5)-2.00*F(1,1)*F(2,5)-6.00*F(1,5)*
2F(3,1)-2.00*F(1,5)*F(2,1)+2.00*F(1,1)*F(1,5)
RETURN
END

```